HHS Public Access

Author manuscript

Acta Biomater. Author manuscript; available in PMC 2023 February 14.

Published in final edited form as:

Acta Biomater. 2022 April 15; 143: 295–309. doi:10.1016/j.actbio.2022.03.021.

Delivery of VEGF and delta-like 4 to synergistically regenerate capillaries and arterioles in ischemic limbs

Hong Niu[a,b,c], **Ning Gao**[a,d], **Yu Dang**[a,d], **Ya Guan**[a,d], **Jianjun Guan**[a,b,c,d,*]

[a]Department of Mechanical Engineering and Materials Science, Washington University in St. Louis. St. Louis, MO, 63130, United States

[b]Center of Regenerative Medicine, Washington University in St. Louis. St. Louis, MO, 63130, United States

[c]Department of Materials Science and Engineering, Ohio State University. Columbus, OH, 43210, United States

[d]Institute of Materials Science and Engineering, Washington University in St. Louis. St. Louis, MO, 63130, United States

Abstract

Vascularization of the poorly vascularized limbs affected by critical limb ischemia (CLI) is necessary to salvage the limbs and avoid amputation. Effective vascularization requires forming not only capillaries, but also arterioles and vessel branching. These processes rely on the survival, migration and morphogenesis of endothelial cells in the ischemic limbs. Yet endothelial cell functions are impaired by the upregulated TGFβ. Herein, we developed an injectable hydrogel-based drug release system capable of delivering both VEGF and Dll4 to synergistically restore endothelial cellular functions, leading to accelerated formation of capillaries, arterioles and vessel branching. In vitro, the Dll4 and VEGF synergistically promoted the human arterial endothelial cell (HAEC) survival, migration, and formation of filopodial structure, lumens, and branches under the elevated TGFβ1 condition mimicking that of the ischemic limbs. The synergistic effect was resulted from activating VEGFR2, Notch-1 and Erk1/2 signaling pathways. After delivering the Dll4 and VEGF via an injectable and thermosensitive hydrogel to the ischemic mouse hindlimbs, 95% of blood perfusion was restored at day 14, significantly higher than delivery of Dll4 or VEGF only. The released Dll4 and VEGF significantly increased density of capillaries and arterioles, vessel branching point density, and proliferating cell density. Besides, the delivery of Dll4 and VEGF stimulated skeletal muscle regeneration and improved muscle function.

*Corresponding author at: Department of Mechanical Engineering and Materials Science, Washington University in St. Louis, 303F Jubel Hall (Office), 340 Whitaker Hall (Lab), Campus Box 1185, One Brookings Drive, St. Louis, MO 63130. jguan22@wustl.edu (J. Guan).

Credit author statement

H.N. and J.G. designed the study. H.N., N.G., Y.G. and Y.D. performed experiments. H.N. and J.G. analyzed the results and wrote the manuscript.

Declaration of Competing Interest

The authors declare no conflict of interest.

Supplementary materials

Supplementary material associated with this article can be found, in the online version, at doi:10.1016/j.actbio.2022.03.021.

Overall, the developed hydrogel-based Dll4 and VEGF delivery system promoted ischemic limb vascularization and muscle regeneration.

Statement of significance—Effective vascularization of the poorly vascularized limbs affected by critical limb ischemia (CLI) requires forming not only capillaries, but also arterioles and vessel branching. These processes rely on the survival, migration and morphogenesis of endothelial cells. Yet endothelial cell functions are impaired by the upregulated TGFβ in the ischemic limbs. Herein, we developed an injectable hydrogel-based drug release system capable of delivering both VEGF and Dll4 to synergistically restore endothelial cell functions, leading to accelerated formation of capillaries, arterioles and vessel branching.

Keywords

Ischemic limb; Capillary; Arteriole; Vessel branching; Vascularization; Skeletal muscle regeneration

1. Introduction

Peripheral artery disease (PAD) is one of the leading causes of morbidity and mortality globally [1,2]. The main pathophysiologic features of PAD are the narrowing of blood vessels and vascular blockage. Critical limb ischemia (CLI) is a serious manifestation of PAD, which is associated with a high risk of limb amputation [3]. Restoration of blood perfusion in the diseased limbs represents the primary treatment goal [4,5]. Currently, surgical procedures for the CLI treatment include lower extremity bypass and endovascular therapy. Yet, these procedures cannot regenerate the damaged vasculature [6-8]. In addition, not all patients are eligible to receive these procedures [9-11]. There is a critical need for strategies that can effectively regenerate vasculature in ischemic limbs leading to restoration of blood flow.

Various therapeutic approaches have been developed to vascularize ischemic limbs, mainly including stem cell therapy, cell secretome therapy, and angiogenic growth factor therapy. In stem cell therapy, stem cells are injected into ischemic limbs with or without using biomaterials as carriers [12,13]. One of the benefits of using biomaterials is that cell retention and survival may be improved. Growing evidence has shown that the delivered cells mostly contribute paracrine effects for vascularization, while some cells may also differentiate into endothelial cells (ECs) and vascular supporting cells [14,15]. Yet, widespread clinical use of stem cell therapy is hampered by intrinsic limitations such as lack of ready-to-use convenience, limited efficacy in a prolonged study period [16-18]. Alternatively, stem cell secretome has been used for ischemic limb treatment [19-21]. Various studies have demonstrated that stem cell secretome delivered into ischemic limbs promoted angiogenesis [22-31]. However, limited reproducibility and difficulty in large-scale production should be tackled before realizing the translation from bench to bed [32]. Extensive studies have focused on delivering angiogenic growth factors for vascularization in the ischemic limb. In both clinical trials and preclinical animal models, the administration of vascular endothelial growth factor (VEGF) [33-35], hepatocyte growth factor (HGF) [36-38], and fibroblast growth factor-1 (FGF-2) [39-41], have shown encouraging results in promoting new vasculature development. Yet the efficacy of current angiogenic growth

factor therapy is limited, and remains unsatisfactory for wide applications in clinics. This is likely due to the delivered growth factors mostly stimulating capillary formation [42-44]. Functional recovery of blood perfusion requires not only capillaries but also other vessels such as arterioles. In addition, current angiogenic growth factor therapy typically delivers single growth factor, while more growth factors are necessary for the formation of both capillaries and arterioles [35,38,39].

In this study, we aimed to regenerate both capillaries and arterioles in ischemic limbs for quicker improvement of blood flow. We delivered hydrogel capable of gradually releasing VEGF and Delta-like 4 (Dll4) into ischemic limbs. VEGF is intricately associated with vascular EC function through binding to VEGF receptor 2 (VEGFR2). VEGFR2 is also robustly exhibited by arterial ECs [45]. Dll4 modulates arteriole formation as it controls artery branching by regulating VEGFR2 expression through Dll4/Notch signaling and inducing a gradient of VEGF signaling [46-50]. Thus, we hypothesized that VEGF and Dll4 can act synergistically to regenerate capillaries and arterioles. The formation of capillaries and arterioles in ischemic limbs is also dependent on the survival, migration, and morphogenesis of arterial ECs. Yet these functions are impaired by the upregulated transforming growth factor beta (TGFβ) [51-55]. We investigated how VEGF and Dll4 regulate endothelial cell functions under ischemic and TGFβ conditions, leading to accelerated vascularization in ischemic limbs.

2. Materials and methods

2.1. Materials

N-Isopropylacrylamide (NIPAAm, TCI) was recrystallized by hexane/ethyl acetate for 3 times. 2-Hydroxyethyl methacrylate (HEMA, Alfa Aesar) was purified by an inhibitor removal column. Benzoyl peroxide (BPO, Fisher Scientific) was used as an initiator for polymerization after lyophilization. Acryloyl chloride (Sigma), 4-(hydroxymethyl)-phenylboronic acid pinacol ester (HPPE, Sigma), triethylamine (TEA, VWR), fetal bovine serum (FBS, Life Technologies), and 1% penicillin-streptomycin (PS, Life Technologies) were used as received. Recombinant human TGFβ1, recombinant human Dll4, and recombinant human VEGF were purchased from Peprotech Inc.

2.2. Cell culture, proliferation, and migration assay

Human arterial endothelial cells (HAECs, Cell Systems) were cultured in T-75 cell culture flasks using basal growth medium supplemented with 10% FBS and 1% PS. The cells were incubated at 37° C with 5% CO_2 and 21% O_2. The medium was changed every other day. The cells were passaged using 0.25% trypsin-EDTA (Life Technologies) when the confluency was 80-90%. The cells of passages 3 to 7 were used for studies.

HAEC migration was investigated by performing a 2D scratch assay [56,57]. The cells were cultured in 6-well plates to reach a confluency of 90-95%. A 200 μL pipet tip was used to scrape the cells in a straight line. Cell debris and extant medium were then removed followed by adding serum-free medium with 20 ng/ml Dll4, 20 ng/ml VEGF, or both. To mimic the condition of elevated TGFβ in CLI, 5 ng/ml TGFβ1 was supplemented during

the culture [58,59]. The wells were imaged at baseline (0 hour) and 24 hours using a light microscope. The distance between the two sides of the scratch was measured using ImageJ. The migration ratio was calculated as:

$$Migration\ ratio = \frac{\text{Interval at 0 hours} - \text{interval at 24 hours}}{\text{Interval at 0 hours}} \times 100\,\%$$

For studying cell survival and proliferation, HAECs were seeded in 96-well plates, and cultured using basal medium with 2% FBS. 20 ng/ml Dll4, 20 ng/ml VEGF, or both were added to the medium. 5 ng/ml TGFβ1 was also added. After 3 days, a PicoGreen dsDNA Quantitation assay (Life Technologies) was performed to quantify cell dsDNA content [60,61]. To image live cells, HAECs were prelabeled with live-cell tracker CMFDA (Life Technologies) before seeding. The cells were imaged using a confocal microscope (Olympus FV1200).

2.3. In vitro studies of endothelial cell filopodial bursts, tube formation, and branch density

HAECs were cultured in a 3D collagen model as described previously [62]. In brief, rat type I soluble collagen (Life Technologies), 10% FBS, Dulbecco's Modified Eagle's Medium (DMEM), and 1 M NaOH were mixed thoroughly. The mixture was then transferred into a 48-well plate and incubated in a 37 °C incubator. After gelation for 30 minutes, 150 μL cell suspension at a density of 8×10^4 cells/mL with different treatments, including TGFβ1 (5 ng/mL); Dll4 (20 ng/mL) and TGFβ; VEGF (20 ng/mL) and TGFβ; or Dll4 and VEGF with TGFβ, was injected into the collagen gel. Four injections were made for each collagen gel. The constructs were incubated at 37 ° C with 5% CO_2 and 21% O_2 for 5 days.

To determine filopodial bursts and tube formation, the collagen constructs were fixed with 4% paraformaldehyde (PFA). Cells in the constructs were visualized using a confocal microscope after von Willebrand factor (vWF) and DRAQ5 staining. To determine branching density, the cells were stained with F-actin and DAPI before imaging. The densities of filopodial structure, lumens, and branches were calculated based on 8 images of each construct, and 4 constructs for each group.

2.4. Protein and gene expression for in vitro cultured cells and in vivo tissue samples

To characterize protein expression, protein lysates from in vitro cultured cells or in vivo tissue samples were collected using RIPA lysis buffer containing protease and phosphatase inhibitors. Protein samples were separated by stain-free precast gels (Bio-rad) and transferred onto low-fluorescence polyvinylidene fluoride (PVDF) membrane. The blots were reacted with anti-VEGFR2 (1:800, Cell Signaling, 2479), anti-Notch-1 (1:600, Cell Signaling, 3608), p44/42 MAPK (t-Erk1/2, 1:10 00, Cell Signaling, 9102) and phospho-p44/42 MAPK (p-Erk1/2, 1:100 0, Cell Signaling, 9101). GAPDH (1:30 00, Cell Signaling, 5174) was served as a loading control antibody. After washing, the blots were incubated with HRP-conjugated secondary antibodies (Life Technologies), followed by detection using WesternBright HRP substrate kit (Advansta). The blots were finally imaged by ChemiDoc XPS system (Bio-rad).

RNA was isolated from tissue samples using TRIzol according to the manufacture's protocol. RNA concentration was quantified by a NanoDrop. cDNA synthesis was conducted using a high-capacity cDNA reverse transcription kit (Life Technologies) on a Mastercycler (Eppendorf). Gene expression was determined by real-time RT-PCR using SYBR Green (Invitrogen) on a PCR instrument (Applied Biosystems). The selected primer pairs are listed in Table S1. β-actin was served as a housekeeping gene. Data were analyzed using the ΔΔCt method [63].

2.5. Release kinetics of Dll4 and VEGF encapsulated in an injectable gel

An injectable, thermosensitive, and fast gelation hydrogel developed in our previous study [57] was used to deliver Dll4 and VEGF into ischemic limbs. The hydrogel was based on NIPAAm, HEMA, and acrylated HPPE (AHPPE), and synthesized by free radical polymerization using BPO as the initiator [57]. The molecular weight of the polymer was measured by gel permeation chromatography (GPC) with a refractive index detector (Wyatt Tech). Dimethylformamide and polystyrene were used as solvent and calibration standards, respectively. The hydrogel solution was prepared by dissolving the polymer in Dulbecco's phosphate-buffered saline (DPBS) at 4 °C overnight. Heparin (1 mg/ml, HP) was then added to the solution. The gelation time of the 4 °C solution was evaluated at 37 °C following our previously established protocols [60]. Briefly, an Olympus microscope (IX71) equipped with a temperature control system was pre-warmed to 37 °C. A drop of 4 °C hydrogel solution was quickly placed on the glass slide sitting on the stage of the microscope. The time for the light to be completely blocked due to forming opaque gel was defined as gelation time. The injectability of the hydrogel was examined by injecting the 4 °C hydrogel solution through a 27-gauge needle without blocking the needle [60].

Rheological test of the hydrogel solution was performed using an AR-G2 rheometer equipped with a Peltier plate. The geometry was 20 mm in radius, and the gap was set as 1 mm. The strain and oscillatory frequency were 2% and 1 Hz, respectively. The testing temperature was swept from 10 °C to 37 °C at a rate of 1 °C/min. The viscosity of 4 °C hydrogel solution/HP was measured with a shear rate sweep from 1 to 20 s^{-1}. The data was analyzed using TA Advantage software.

To load Dll4 and VEGF into the hydrogel, Dll4 and VEGF were first dissolved in DPBS at the concentrations of 20 μg/mL and 10 μg/mL, respectively. The individual solutions or both were then mixed with the hydrogel solution. The mixture (200 μL) was transferred to a 1.5 mL low protein binding centrifuge tube (Life technologies). After 4 hours of incubation at 37 °C to reach the equilibrium state of the hydrogel, the supernatant was removed followed by adding a 200 μL release medium (DPBS with 1% penicillin). The hydrogel was immersed in the release medium with only bottom touching the centrifuge tube. The tubes (n=6 for each group) were incubated at 37 °C for 14 days. At days 1, 3, 5, 7, 10, and 14, the release medium was collected and stored at −80 °C, and was replaced with 200 μL of fresh release medium. The concentration of Dll4 not being encapsulated in the hydrogel and released from the hydrogel was determined using anti-human Dll4 antibody (Peprotech, 500-P279) with biotinylated anti-human sDll4 (Peprotech, 500-P279BT) [64]. The VEGF concentration was measured using a VEGF ELISA development kit (Peprotech, 900-K10).

The cumulative release ratio was calculated based on the amount of growth factor released, and the amount of growth factor remained in the hydrogel at the beginning of the release study.

2.6. Critical limb ischemia mouse model

All animal care and experimental procedures were performed according to the guidelines of the National Institutes of Health, and approved by the Institutional Animal Care and Use Committee of Washington University in St. Louis. Critical limb ischemia surgery was performed on 8-week-old, female C57BL/6J mice (Jackson Laboratory). For each mouse, ischemia was induced on one hindlimb by the ligation of both unilateral femoral arteries and veins [61,65]. The contralateral hindlimb was used as a control. Thirty minutes after ligation, intramuscular injections were performed to the gracilis muscle on the ischemic hindlimb (50 μL/injection, and 3 injections each hindlimb). The study groups included surgery only (Surgery only), hydrogel treatment alone (Gel only), hydrogel with 20 μg/mL Dll4 (Dll4/Gel), hydrogel with 10 μg/mL VEGF (VEGF/Gel), and hydrogel with 20 μg/mL Dll4 and VEGF 10 μg/mL (Dll/VEGF/Gel). Eight mice were used for each group.

2.7. Blood perfusion, ischemia scoring, and treadmill test

Blood perfusion of hindlimbs was monitored using a laser Doppler perfusion imager (Perimed) after injection, and at days 7, and 14. The ratio of blood perfusion between the surgery hindlimb and the contralateral hindlimb at each time was quantified [61,65]. The mice were also evaluated in terms of ischemia score that assesses the degree of digital amputation, necrosis, and cyanosis compared to the control contralateral hindlimb. The evaluation was based on an established seven-point ischemia score scale with modification (Table S2) [66,67]. The hindlimbs before surgery were set as a score of seven.

The running ability of the mice was determined by a treadmill test [68,69]. The mice were trained to use the treadmill (Cambridge Technology Inc.) 7 days before the surgery. The training was continued for 15 minutes per day at a speed of 120 m/min. After surgery and at days 7 and 14, the mice were placed on the lanes of the treadmill for warm training at a speed of 70 m/min for 30 minutes, followed by a testing speed of 120 m/min. The time of exhaustion for each mouse (falling from the lane three continuous times) was recorded. Running distance was determined by the exhaustion time and speed.

2.8. Histological and immunohistochemistry staining

Fourteen days post-injection, mice were euthanized, and hindlimb tissue samples were collected. The tissues were fixed in 4% PFA, embedded in paraffin, and sectioned at 10 μm. H&E staining was performed, and the images were taken by an inverted light microscope (Olympus) to evaluate muscle degeneration, muscle fiber diameter, and central nuclei density. Immunohistochemistry staining (IHC) was performed to characterize blood vessels using isolectin GS-IB4 (Invitrogen, I21414) and mouse anti-alpha-smooth muscle actin (α-SMA) (Abcam, ab7817), arteriole density using anti-ephrinB2 (Santa Cruz, sc-398735), proliferating cells using rat anti-Ki67 (Invitrogen, 14-5698-82), and inflammatory cells using rat anti-CD68 antibody (Abcam, ab534 4 4). After incubating with primary antibodies overnight, the corresponding secondary antibodies were applied for 1 hour. Cell nuclei were

stained with DAPI. The tissue slices were then imaged by a confocal microscope. The quantifications were performed using ImageJ (n≥6 for each group).

2.9. Characterization of blood vessel branching

To determine blood vessel branching, vascular perfusion with FITC-conjugated isolectin B4 and anti-α-SMA was performed on day14 [61]. The ischemic hindlimbs were then collected, and cryosectioned in sagittal orientation with a thickness of 10 μm. The tissue sections were then imaged using a confocal microscope. The quantification for vessel branching point density was performed based on the obtained images (n≥6 for each group).

2.10. Statistical analysis

Data are presented as mean ± standard deviation. Statistical analysis was performed using one-way ANOVA with Tukey's posthoc test. Significance was defined as $p<0.05$.

3. Results and discussion

3.1. Dll4 and VEGF synergistically improved migration and survival of HAECs impaired by TGFβ

Regeneration of capillaries and arterioles is necessary for rebuilding vasculature in the ischemic limbs during vascularization therapy. Yet the impaired EC migration, survival, and morphogenesis in the ischemic limbs impede the vascularization process [70-72]. One of the major causes of EC dysfunction is upregulated TGFβ [52,73]. While TGFβ plays an essential role in modulating cell migration and morphogenesis, the overexpression of TGFβ observed in CLI decreases the migration and morphogenesis of ECs [73,74]. In this work, we investigated whether co-delivery of VEGF and Dll4 can improve TGFβ-impaired EC function and accelerate the formation of both capillaries and arterioles in ischemic limbs. Previous studies have revealed that VEGF/VEGFR2 signaling boosts endothelial motility, filopodia extension, and proliferation required for vessel formation [75,76]. Dll4/Notch signaling is essential to converting the formed sprouts into tubules and making a connection with other vessels by the proliferated stalk ECs [77,78]. However, it is unclear how VEGF and Dll4 function in a diseased model with an elevated TGFβ level.

We first examined the migration and survival of HAECs in TGFβ conditions. As shown in Fig. 1a and b, we observed a significant increase in migration rates with Dll4 and VEGF singular treatments. Moreover, treating with Dll4 and VEGF showed the highest migration rate among all the groups ($p<0.05$ when "Dll4/VEGF/TGFβ" vs. "Dll4/TGFβ" or "VEGF/TGFβ"; $p<0.001$ when "Dll4/VEGF/TGFβ" vs. "TGFβ" control group).

One crucial inducer for the migration of endothelial cells is filopodia formation, which is essential in probing and sensing other molecular factors in the extracellular matrix (ECM) to guide the direction of the cell movements [79,80]. To investigate the roles of Dll4 and VEGF in modulating arterial EC filopodia formation, we generated a 3D, cell-seeded-collagen model cultured with TGFβ and treated with Dll4/VEGF. In Fig. 1c and d, HAECs treated with VEGF/TGFβ and Dll4/TGFβ exhibited 46% and 73% increased formation of filopodial burst structure, respectively, compared to TGFβ treatment alone. Notably, the group of Dll4/

VEGF/TGFβ led to a more than three-fold increase in the density of filopodial bursts over TGFβ treatment alone and significant increases over Dll4 and VEGF treatments.

The impact of Dll4 and VEGF on the survival of HAECs was examined by live-cell imaging and dsDNA assay (Fig. 1e and f). Compared to TGFβ treatment alone, Dll4-treated and VEGF-treated groups increased in cellularity by 24% and 25%, respectively. The Dll4 and VEGF group further enhanced the survival of HAECs, with an increase of 45% compared to the control group. The above results suggest a synergistic effect of Dll4 and VEGF in promoting TGFβ-impaired HAEC migration and survival.

3.2. Dll4 with VEGF simultaneously enhanced the lumen formation, and branching of HAECs

To investigate how Dll4 and VEGF modulate HAECs sprouting and lumen formation under TGFβ condition, we seeded HAECs in a 3D-collagen model, cultured in the medium with TGFβ1, and treated with Dll4, VEGF, or both. After 3 days of incubation, the cells treated with Dll4 or VEGF formed significantly higher density of lumen-like structures compared to the cells in the TGFβ group (Fig. 2a and c). The lumen density in the group with Dll4/VEGF treatment was further significantly increased ($p<0.001$, Dll4/VEGF/TGFβ vs. Dll4/TGFβ, and Dll4/VEGF/TGFβ vs. VEGF/TGFβ), indicating a synergistic effect between Dll4 and VEGF in inducing sprouting and in vitro angiogenesis of HAECs.

We also assessed the branching behavior of HAECs (Fig. 2b and d). Both Dll4 and VEGF significantly increased HAEC branching density compared to TGFβ alone group. Of note, the Dll4/TGFβ group more pronouncedly enhanced the branching of HAECs than the VEGF/TGFβ group. The Dll4/VEGF/TGFβ treatment group demonstrated a significantly higher branching density than all other treatment groups ($p<0.001$). These data demonstrate that Dll4 plays a critical role in HAECs forming branches, and can be further increased with the supplementation of VEGF.

3.3. Synergistic effect of Dll4 and VEGF in re-activating VEGF/VEGFR2 and Dll4/Notch signaling pathways under TGFβ

To investigate how Dll4 and VEGF regulated VEGFR2 and Notch signaling pathways under TGFβ condition leading to enhanced HAEC survival, migration, and morphogenesis, we examined the expression of VEGFR2 and Notch-1 at protein levels. Treatment of TGFβ1 decreased expression of VEGFR2 compared with no TGFβ group (Fig. 3). The decrease in VEGFR2 expression was abrogated by the addition of VEGF and further abolished with the involvement of Dll4 (Fig. 3). The decreased VEGFR2 by TGFβ caused the inhibition of Notch-1 and deactivation of subsequent MAPK/ERK1/2 cascade [81]. Notch-1 and phosphorated Erk1/2 (p-Erk1/2) expression was upregulated by the treatment of either Dll4 or VEGF and was further upregulated when treated with a combination of Dll4 and VEGF (Fig. 3). Overall, these data showed that VEGF/VEGFR2 and Dll4/Notch signaling pathways were deactivated by TGFβ, and synergistically re-activated by the treatments of Dll4 and VEGF in HAECs.

Previous studies have shown that proliferation of endothelial cells was positively correlated with the activation of VEGFR2 and subsequent MAPK/ERK1/2 cascade [81,82], and

activation of Notch signaling stabilizes the formation of lumens by arterial ECs while inhibition of this pathway blocks the network formation [78,83]. Consistent with these previous studies, we demonstrate that Dll4 and VEGF-upregulated VEGFR2 and Notch-1 expressions led to a significant impact on the proliferation and morphogenesis of HAECs (Fig. 3).

3.4. Sustained release with maintained bioactivity of VEGF and Dll4 encapsulated in hydrogel

To deliver Dll4 and VEGF to ischemic limbs and efficiently retain the growth factors in the tissue, a thermosensitive and fast gelation hydrogel based on NIPAAm, HEMA, and AHPPE was used as a carrier. Our previous study demonstrated that the polymer synthesized from NIPAAm, HEMA, and AHPPE exhibited good biocompatibility [57]. The obtained polymer had number average molecular weight of 1.8×10^4 g/mol and a PDI of 1.4. The hydrogel solution (6 wt.% in DPBS) had a gelation temperature of 17 °C based on the rheological test (Fig. 4a). After incubation in 37 °C DPBS for 4 weeks, the hydrogel exhibited a weight loss of 8%. To stabilize the growth factors, HP was mixed with the hydrogel. The resulting solution was flowable at 4 °C (Fig. 4b), and can be readily injected through a 27G needle at this temperature (Fig. 4c). The 4 °C solution also exhibited shear thinning behavior where viscosity was decreased with the increase of shear rate (Fig. 4d). After transferring the 4 °C solution to 37 °C condition, it solidified in 6 s and formed a solid gel (Fig. 4e). The use of fast gelation hydrogel for growth factor delivery is advantageous as it can quickly solidify upon injection into ischemic limbs, thus largely retaining the encapsulated growth factors in the tissue, and minimizing growth factor loss due to leaking of the injected hydrogel.

The release studies for Dll4 and VEGF were conducted in 37 °C DPBS where the hydrogel was immersed in the DPBS (Fig. 4f). Dll4 and VEGF were encapsulated in the hydrogel at a loading efficiency of 80% and 83%, respectively (Fig. 4g & h). Both growth factors were released continuously from the hydrogel over a 14-day period (Fig. 4g & h). The Dll4 and VEGF were released faster from the hydrogel encapsulated with individual growth factor than that encapsulated with both growth factors. The sustained release of Dll4 and VEGF is likely due to their interaction with the NIPAAm-based hydrogel by hydrogen bonding between amide groups [62]. When both VEGF and Dll4 were encapsulated in the hydrogel, the interaction between the two growth factors including hydrogen bonding and electrostatic interaction further retained them in the hydrogel, leading to delayed-release. Overall, these results demonstrate that the hydrogel carrier is capable of sustainedly releasing Dll4 and VEGF. After implantation into ischemic hindlimbs, the Dll4 and VEGF may release faster as the weight loss rate of the hydrogel may be higher due to reactive oxygen species in the tissue environment [57].

3.5. Delivery of Dll4 and VEGF stimulated blood flow recovery and alleviated severity of ischemia in the operated hindlimbs of mice

To determine the efficacy of delivery of Dll4 and VEGF in promoting vascularization in ischemic limbs, the 4 °C hydrogel encapsulated with Dll4 (Dll4/Gel), VEGF (VEGF/Gel), or Dll4 and VEGF (Dll4/VEGF/Gel) were injected in the ischemic region after induction of ischemia (Fig. 5a). The injected hydrogel did not leak out during and after the injection. On

day 0, the blood perfusion in the operated limbs was 10-12% of the contralateral limb as examined by laser Doppler imaging system. During the following 14-day treatment period, the blood perfusion for the surgery group without hydrogel treatment (Surgery group) slowly increased to 38% of the contralateral control limb. The injection of hydrogel alone (Gel group) largely increased blood perfusion compared to the Surgery group, with 58% of blood perfusion at day 14 (Fig. 5b and c). The injection of Dll4/Gel and VEGF/Gel groups significantly increased blood perfusion compared to the Gel group, with 72% and 76% of blood perfusion recovery at day 14, respectively ($p<0.05$, Dll4/Gel group vs. Gel group; $p<0.05$, VEGF/Gel group vs. Gel group). The delivery of both Dll4 and VEGF (Dll4/VEGF/Gel group) synergistically further increased blood perfusion with 98% of blood perfusion recovery at day 14 (Fig. 5c). Consistent with blood perfusion results, the modified ischemia score gradually augmented during the 14-day treatment period where a greater score represents lower ischemia (Fig. 5d). The group treated with Dll4/VEGF/Gel demonstrated the highest modified ischemic score (Fig. 5d).

3.6. Dll4 and VEGF delivery enhanced blood vessel formation, arteriole formation, and vessel branching with enhanced expression of VEGFR2, Notch-1, and p-Erk1/2

To visualize the blood vessel formation in vivo, tissue sections were stained with isolectin and α-SMA. The two markers are for endothelial cells and vascular smooth muscle cells, respectively. There were few capillaries in the surgery only group, and a slightly higher density of vessels with the injection of the hydrogel (Fig. 6a). The vessel density in Dll4/Gel group was increased near two-fold compared to that of the hydrogel alone group (Fig. 6c). The VEGF/Gel group exhibited a significantly higher vessel density than the Dll4/Gel group ($p<0.01$). The highest vessel density was found in the Dll4/VEGF/Gel group, which was increased more than three-fold compared to the Gel group ($p<0.001$), and significantly higher than that of the Dll4/Gel group ($p<0.001$) or VEGF/Gel group ($p<0.01$). The delivery of Dll4 and VEGF also regenerated mature blood vessels where the Dll4/VEGF/Gel group had the highest density of vessels with isolectin$^+$ ECs and α-SMA+ smooth muscle cells (Fig. 6d).

To further evaluate whether delivery of VEGF and Dll4 promoted arteriole formation, EphrinB2 staining, a marker specifically for arterial endothelial cells, was performed (Fig. 6b). The delivered Dll4 and VEGF stimulated arteriole formation. The ischemic limbs injected with Dll4/Gel and VEGF/Gel groups showed significantly greater arteriole density than the ischemic limbs injected with hydrogel only ($p<0.01$, Fig. 6e). The Dll4 and VEGF released from the hydrogel demonstrated similar capability in promoting arteriole formation. Notably, the combined delivery of Dll4 and VEGF synergistically enhanced arteriole formation ($p<0.01$).

Dll4 has been demonstrated to induce vessel branching [49,84]. To determine how released Dll4 stimulated vessel branching, we performed vascular perfusion with fluorescent-labeled antibodies isolectin and α-SMA, and sectioned ischemic limbs in the sagittal direction (Fig. 6f). The Dll4/Gel and Dll4/VEGF/Gel groups formed a greater number of vessel branches than the Surgery, Gel, and VEGF/Gel groups (Fig. 6f). Quantitatively, these two groups

exhibited substantially higher branching point density, and the Dll4/VEGF/Gel groups had the highest branching point density (Fig. 6g).

The above results demonstrate that sustained delivery of Dll4 and VEGF promoted capillary and arteriole formation, vessel maturation, and vessel branching in ischemic limbs. In addition, Dll4 and VEGF showed synergistic effects in these processes. Based on the in vitro studies, the facilitation of vascularization is likely because of: (1) Dll4 and VEGF increasing survival and migration of ECs under upregulated TGFβ condition of ischemic limbs (Fig. 1a, b, e, and f), and (2) increased tube formation of ECs stimulated by Dll4 and VEGF (Fig. 2a and c).

Akin to the in vitro mechanism proved in Fig. 3, we extracted the proteins from tissue samples at day 14 to examine the effects of Dll4 and VEGF released in vivo on VEGFR2, Notch, and Erk1/2 signaling. Consistent with the in vitro findings, the expression of VEGFR2, Notch-1, and p-Erk1/2 was substantially upregulated in the Dll4/VEGF/Gel group at day 14 (Fig. 6h) compared to the other treatment groups. Mechanistically, for both our in vitro and in vivo data, we delineated that the synergistic effect of Dll4 and VEGF under elevated TGFβ condition is due to activating VEGFR2 and Notch signaling pathways. Additionally, the activation of the VEGFR2 signaling pathway likely induced an upregulation of p-Erk1/2 (Fig. 6h), which is a major downstream cascade of MAPK signaling and is required for the integrity of ECs during angiogenesis [85,86].

3.7. Dll4 and VEGF had a synergistic effect in promoting host cell survival without causing inflammation in vivo

As the in vitro efficacy of Dll4 and VEGF in promoting HAEC proliferation was prominent (Fig. 1e and f), the consequent behavior of rescuing host cells in vivo was examined using a proliferating cell marker Ki67 [61,87] (Fig. 7a and c). The Dll4/Gel and VEGF/Gel groups displayed significantly higher $Ki67^+$ cell density than the Surgery and Gel groups ($p<0.05$) at day 14. There was no significant difference between the Dll4/Gel and VEGF/Gel groups ($p>0.05$), while host cells were able to proliferate more with the delivery of Dll4/VEGF/Gel group ($p<0.01$). Notably, the Gel group exhibited a significantly greater density of Ki67+ cells than the Surgery group ($p<0.05$), possibly because the hydrogel scavenged ROS in the ischemic limbs and decreased ROS attack-induced cell death.

To investigate potential tissue inflammation resulting from the injection of growth factor-encapsulated hydrogel solutions, CD68 staining was performed (Fig. 7b and d) on the tissue samples collected on day 14. Compared with the Surgery group, the injection groups had a similar $CD68^+$ cell density, indicating that the injected growth factor and hydrogel did not provoke tissue inflammation. Interestingly, the expressions of pro-inflammatory genes tumor necrosis factor (*Tnfa*) [88] and interleukin 1 beta (*Il1β*) [89] were significantly reduced in the Dll4/VEGF/Gel group compared with other groups (Fig. 7e and f). These results demonstrate that the combination of Dll4 and VEGF has the potential to decrease inflammation in ischemic tissues. However, it remains to be investigated how Dll4 and VEGF supplementation reduce inflammation in ischemic tissues.

3.8. Improved muscle regeneration and functional recovery by the delivery of Dll4 and VEGF

To determine whether the delivery of Dll4 and VEGF improved the regeneration of skeletal muscle tissues, histological analysis of the tissue harvested on day 14 was conducted. The skeletal muscles in the Surgery group degenerated as muscle fibers were highly separated (Fig. 8a), and had the lowest mean muscle fiber diameters (Fig. 8b), and density of central nuclei (Fig. 8c). The injection of hydrogel slightly alleviated muscle degeneration where the muscle fiber diameter was substantially increased ($p>0.05$ Fig. 8b). In contrast, the Dll4/Gel group and VEGF/Gel group showed a more compact tissue structure with a larger fiber diameter and significantly higher density of central nuclei (Fig. 8b and c).

The delivery of the Dll4/VEGF/Gel group further improved muscle anatomy, and increased fiber diameter (Fig. 8b) and density of central nuclei (Fig. 8c), indicating a synergistic effect in muscle regeneration. The muscle regeneration augmented muscle function. The group treated with Dll4/VEGF/Gel demonstrated the highest running ability (Fig. 8d).

To investigate the underlying mechanism, the gene expression of insulin-like growth factor 1 (*Igf1*) and hepatocyte growth factor (*Hgf*) from tissue samples of different treatments were tested using real-time RT-PCR. *Igf1* promotes myoblast proliferation and differentiation of satellite cells in skeletal muscle [90]. *Hgf* activates quiescent satellite cells to form myoblasts [91,92]. We found that both factors were significantly increased in the group of Dll4/VEGF/Gel group compared to the other groups (Fig. 8e and f).

The above results demonstrate that combined delivery of Dll4 and VEGF enhanced vascularization and skeletal muscle regeneration in ischemic limbs of young wild-type mice. While the results are encouraging, there are limitations on the animal model. First, the growth factors were delivered 30 minutes after ligation of unilateral femoral arteries and veins, before the chronic ischemic condition was established. Second, the CLI model was induced in young wild-type mice instead of aged mice with pre-existing PAD.

In future work, we will test therapeutic efficacy when delivering Dll4 and VEGF into aged mice with PAD after chronic ischemic condition is developed. In this work, we investigated the therapeutic efficacy of controlled release of Dll4, VEGF, or both in regenerating ischemic limbs. We did not examine the therapeutic efficacy when delivering bare Dll4 and VEGF without using hydrogel. We will include these groups in future studies to demonstrate the benefits of controlled release over direct delivery of these growth factors.

4. Conclusion

In this study, we demonstrated that Dll4 and VEGF synergistically promoted endothelial cell survival, migration, and tube formation under evaluated TGFβ mimicking that of ischemic limbs. The upregulated TGFβ in ischemic limbs impairs endothelial cell function leading to delayed vascularization. The synergistic effect of Dll4 and VEGF was resulted from activating VEGFR2, Notch-1, and Erk1/2 signaling pathways. The delivery of Dll4 and VEGF significantly stimulated the capillary and arteriole formation, and vessel branching

in ischemic limbs. In addition, the delivered Dll4 and VEGF promoted skeletal muscle regeneration and increased muscle function.

Supplementary Material

Refer to Web version on PubMed Central for supplementary material.

Acknowledgment

This work was supported by US National Institutes of Health (R01HL138175, R01HL138353, R01EB022018, R01AG056919, and R01AR077616). The confocal images were performed in Washington University Center for Cellular Imaging (WUCCI) supported by Washington University School of Medicine. We would like to acknowledge the editing assistance provided by InPrint: A Scientific Editing Network at Washington University in St. Louis.

References

[1]. Criqui MH, V. Aboyans, Epidemiology of peripheral artery disease, Circulation research 116 (2015) 1509–1526. [PubMed: 25908725]

[2]. Agnelli G, Belch JJ, Baumgartner I, Giovas P, Hoffmann U. Morbidity and mortality associated with atherosclerotic peripheral artery disease: A systematic review, Atherosclerosis 293 (2020) 94–100. [PubMed: 31606132]

[3]. Farber A, Eberhardt RT. The current state of critical limb ischemia: a systematic review, JAMA surgery 151 (2016) 1070–1077. [PubMed: 27551978]

[4]. Goumans MJ, Valdimarsdottir G, Itoh S, Rosendahl A, Sideras P, ten Dijke P. Balancing the activation state of the endothelium via two distinct TGF-β type I receptors, The EMBO journal 21 (2002) 1743–1753. [PubMed: 11927558]

[5]. Uccioli L, Meloni M, Izzo V, Giurato L, Merolla S, Gandini R. Critical limb ischemia: current challenges and future prospects, Vascular health and risk management 14 (2018) 63. [PubMed: 29731636]

[6]. Duscha BD, Robbins JL, Jones WS, Kraus WE, Lye RJ, Sanders JM, Allen JD, Regensteiner JG, Hiatt WR, Annex BH. Angiogenesis in skeletal muscle precede improvements in peak oxygen uptake in peripheral artery disease patients, Arteriosclerosis, thrombosis, and vascular biology 31 (2011) 2742–2748.

[7]. Deguchi J, Shigematsu K, Ota S, Kimura H, Fukayama M, Miyata T. Surgical result of critical limb ischemia due to tibial arterial occlusion in patients with systemic scleroderma, Journal of vascular surgery 49 (2009) 918–923. [PubMed: 19223137]

[8]. Olin JW, White CJ, Armstrong EJ, Kadian-Dodov D, Hiatt WR. Peripheral artery disease: evolving role of exercise, medical therapy, and endovascular options, Journal of the American College of Cardiology 67 (2016) 1338–1357. [PubMed: 26988957]

[9]. Stein R, Hriljac I, Halperin JL, Gustavson SM, Teodorescu V, Olin JW. Limitation of the resting ankle-brachial index in symptomatic patients with peripheral arterial disease, Vascular medicine 11 (2006) 29–33. [PubMed: 16669410]

[10]. Jones WS, Schmit KM, Vemulapalli S, Subherwal S, Patel MR, Hasselblad V, Heidenfelder BL, Chobot MM, Posey R, Wing L. Treatment strategies for patients with peripheral artery disease. 2013.

[11]. Hiramoto JS, Teraa M, de Borst GJ, Conte MS. Interventions for lower extremity peripheral artery disease, Nature Reviews Cardiology 15 (2018) 332–350. [PubMed: 29679023]

[12]. Zhang K, Chen X, Li H, Feng G, Nie Y, Wei Y, Li N, Han Z, Han Z-c, Kong D. A nitric oxide-releasing hydrogel for enhancing the therapeutic effects of mesenchymal stem cell therapy for hindlimb ischemia, Acta biomaterialia 113 (2020) 289–304. [PubMed: 32663662]

[13]. Park I-S, Chung P-S, Ahn JC. Adipose-derived stem cell spheroid treated with low-level light irradiation accelerates spontaneous angiogenesis in mouse model of hindlimb ischemia, Cytotherapy 19 (2017) 1070–1078. [PubMed: 28739168]

[14]. Young SA, Sherman SE, Cooper TT, Brown C, Anjum F, Hess DA, Flynn LE, Amsden BG. Mechanically resilient injectable scaffolds for intramuscular stem cell delivery and cytokine release, Biomaterials 159 (2018) 146–160. [PubMed: 29324306]

[15]. Wang X, Zhang J, Cui W, Fang Y, Li L, Ji S, Mao D, Ke T, Yao X, Ding D. Composite hydrogel modified by IGF-1C domain improves stem cell therapy for limb ischemia, ACS applied materials & interfaces 10 (2018) 4481–4493. [PubMed: 29327586]

[16]. An T, Chen Y, Tu Y, Lin P. Mesenchymal Stromal Cell-Derived Extracellular Vesicles in the Treatment of Diabetic Foot Ulcers: Application and Challenges, Stem cell reviews and reports (2020).

[17]. Jaluvka F, Ihnat P, Madaric J, Vrtkova A, Janosek J, Prochazka V. Current Status of Cell-Based Therapy in Patients with Critical Limb Ischemia, International journal of molecular sciences (2020) 21. [PubMed: 33375030]

[18]. Benoit E, O'Donnell TF Jr, Patel AN. Safety and efficacy of autologous cell therapy in critical limb ischemia: a systematic review, Cell transplantation 22 (2013) 545–562. [PubMed: 22490340]

[19]. Wagner T, Traxler D, Simader E, Beer L, Narzt M-S, Gruber F, Madlener S, Laggner M, Erb M, Vorstandlechner V. Different pro-angiogenic potential of γ-irradiated PBMC-derived secretome and its subfractions, Scientific reports 8 (2018) 1–15. [PubMed: 29311619]

[20]. Takeuchi R, Katagiri W, Endo S, Kobayashi T. Exosomes from conditioned media of bone marrow-derived mesenchymal stem cells promote bone regeneration by enhancing angiogenesis, PLoS One 14 (2019) e0225472. [PubMed: 31751396]

[21]. Ferreira JR, Teixeira GQ, Santos SG, Barbosa MA, Almeida-Porada G, Gonçalves RM. Mesenchymal stromal cell secretome: influencing therapeutic potential by cellular pre-conditioning, Frontiers in immunology 9 (2018) 2837. [PubMed: 30564236]

[22]. W Du, Zhang K, Zhang S, Wang R, Nie Y, Tao H, Han Z, Liang L, Wang D, Liu J, Liu N, Han Z, Kong D, Zhao Q, Li Z. Enhanced proangiogenic potential of mesenchymal stem cell-derived exosomes stimulated by a nitric oxide releasing polymer, Biomaterials 133 (2017) 70–81. [PubMed: 28433939]

[23]. Hu GW, Li Q, Niu X, Hu B, Liu J, Zhou SM, Guo SC, Lang HL, Zhang CQ, Wang Y, Deng ZF. Exosomes secreted by human-induced pluripotent stem cell-derived mesenchymal stem cells attenuate limb ischemia by promoting angiogenesis in mice, Stem cell research & therapy 6 (2015) 10. [PubMed: 26268554]

[24]. Ju C, Li Y, Shen Y, Liu Y, Cai J, Liu N, Ma G, Tang Y. Transplantation of Cardiac Mesenchymal Stem Cell-Derived Exosomes for Angiogenesis, Journal of cardio-vascular translational research 11 (2018) 429–437.

[25]. Mathiyalagan P, Liang Y, Kim D, Misener S, Thorne T, Kamide CE, Klyachko E, Losordo DW, Hajjar RJ, Sahoo S. Angiogenic Mechanisms of Human CD34(+) Stem Cell Exosomes in the Repair of Ischemic Hindlimb, Circulation research 120 (2017) 1466–1476. [PubMed: 28298297]

[26]. Ye M, Ni Q, Qi H, Qian X, Chen J, Guo X, Li M, Zhao Y, Xue G, Deng H, Zhang L. Exosomes Derived from Human Induced Pluripotent Stem Cells-Endothelia Cells Promotes Postnatal Angiogenesis in Mice Bearing Ischemic Limbs, International journal of biological sciences 15 (2019) 158–168. [PubMed: 30662356]

[27]. Zhu Q, Li Q, Niu X, Zhang G, Ling X, Zhang J, Wang Y, Deng Z. Extracellular Vesicles Secreted by Human Urine-Derived Stem Cells Promote Ischemia Repair in a Mouse Model of Hind-Limb Ischemia. Cellular physiology and biochemistry: international journal of experimental cellular physiology, biochemistry, and pharmacology 47 (2018) 1181–1192.

[28]. Anderson JD, Johansson HJ, Graham CS, Vesterlund M, Pham MT, Bramlett CS, Montgomery EN, Mellema MS, Bardini RL, Contreras Z, Hoon M, Bauer G, Fink KD, Fury B, Hendrix KJ, Chedin F, El-Andaloussi S, Hwang B, Mulligan MS, Lehtiö J, Nolta JA. Comprehensive Proteomic Analysis of Mesenchymal Stem Cell Exosomes Reveals Modulation of Angiogenesis via Nuclear Factor-KappaB Signaling, Stem Cells 34 (2016) 601–613. [PubMed: 26782178]

[29]. Yan B, Zhang Y, Liang C, Liu B, Ding F, Wang Y, Zhu B, Zhao R, Yu XY, Li Y. Stem cell-derived exosomes prevent pyroptosis and repair ischemic muscle injury through a novel exosome/circHIPK3/FOXO3a pathway, Theranostics 10 (2020) 6728–6742. [PubMed: 32550900]

[30]. Johnson TK, Zhao L, Zhu D, Wang Y, Xiao Y, Oguljahan B, Zhao X, Kirlin WG, Yin L, Chilian WM, Liu D. Exosomes derived from induced vascular progenitor cells promote angiogenesis in vitro and in an in vivo rat hindlimb ischemia model, American journal of physiology Heart and circulatory physiology 317 (2019) H765–h76. [PubMed: 31418583]

[31]. Zhu D, Johnson TK, Wang Y, Thomas M, Huynh K, Yang Q, Bond VC, Chen YE, Liu D. Macrophage M2 polarization induced by exosomes from adipose-derived stem cells contributes to the exosomal proangiogenic effect on mouse ischemic hindlimb, Stem cell research & therapy 11 (2020) 162. [PubMed: 32321589]

[32]. Andriolo G, Provasi E, Lo Cicero V, Brambilla A, Soncin S, Torre T, Milano G, Biemmi V, Vassalli G, Turchetto L. Exosomes from human cardiac progenitor cells for therapeutic applications: development of a GMP-grade manufacturing method, Frontiers in physiology 9 (2018) 1169. [PubMed: 30197601]

[33]. Choksy S, Pockley A, Wajeh Y, Chan P. VEGF and VEGF receptor expression in human chronic critical limb ischaemia, European journal of vascular and endovascular surgery 28 (2004) 660–669. [PubMed: 15531204]

[34]. Rajagopalan S, Shah M, Luciano A, Crystal R, Nabel EG. Adenovirus-mediated gene transfer of VEGF121 improves lower-extremity endothelial function and flow reserve, Circulation 104 (2001) 753–755. [PubMed: 11502697]

[35]. Yu Z, Witman N, Wang W, Li D, Yan B, Deng M, Wang X, Wang H, Zhou G, Liu W. Cell-mediated delivery of VEGF modified mRNA enhances blood vessel regeneration and ameliorates murine critical limb ischemia, Journal of Controlled Release 310 (2019) 103–114. [PubMed: 31425721]

[36]. Barć P, Antkiewicz M, Śliwa B, Baczyńska D, Witkiewicz W, Skóra JP. Treatment of critical limb ischemia by pIRES/VEGF165/HGF administration, Annals of vascular surgery 60 (2019) 346–354. [PubMed: 31200059]

[37]. Slobodkina E, Boldyreva M, Karagyaur M, Eremichev R, Alexandrushkina N, Balabanyan V, Akopyan Z, Parfyonova Y, Tkachuk V, Makarevich P. Therapeutic Angiogenesis by a “Dynamic Duo”: Simultaneous Expression of HGF and VEGF165 by Novel Bicistronic Plasmid Restores Blood Flow in Ischemic Skeletal Muscle, Pharmaceutics 12 (2020) 1231. [PubMed: 33353116]

[38]. Wang L-S, H Wang Q-L Zhang, Yang Z-J, Kong F-X, Wu C-T. Hepatocyte growth factor gene therapy for ischemic diseases, Human gene therapy 29 (2018) 413–423. [PubMed: 29409352]

[39]. Das S, Monteforte AJ, Singh G, Majid M, Sherman MB, Dunn AK, Baker AB. Syndecan-4 Enhances Therapeutic Angiogenesis after Hind Limb Ischemia in Mice with Type 2 Diabetes, Advanced healthcare materials 5 (2016) 1008–1013. [PubMed: 26891081]

[40]. T Yin, He S, Su C, Chen X, Zhang D, Wan Y, Ye T, Shen G, Wang Y, Shi H. Genetically modified human placenta–derived mesenchymal stem cells with FGF–2 and PDGF–BB enhance neovascularization in a model of hindlimb ischemia, Molecular Medicine Reports 12 (2015) 5093–5099. [PubMed: 26239842]

[41]. Cartland SP, Genner SW, Zahoor A, Kavurma MM. Comparative evaluation of TRAIL, FGF-2 and VEGF-A-induced angiogenesis in vitro and in vivo, International journal of molecular sciences 17 (2016) 2025. [PubMed: 27918462]

[42]. Kumar VA, Liu Q, Wickremasinghe NC, Shi S, Cornwright TT, Deng Y, Azares A, Moore AN, Acevedo-Jake AM, Agudo NR. Treatment of hind limb ischemia using angiogenic peptide nanofibers, Biomaterials 98 (2016) 113–119. [PubMed: 27182813]

[43]. You J, Sun J, Ma T, Yang Z, Wang X, Zhang Z, Li J, Wang L, Ii M, Yang J. Curcumin induces therapeutic angiogenesis in a diabetic mouse hindlimb ischemia model via modulating the function of endothelial progenitor cells, Stem cell research & therapy 8 (2017) 1–10. [PubMed: 28057078]

[44]. Cho B-R, Ryu DR, Lee K-S, Lee D-K, Bae S, Kang DG, Ke Q, Singh SS, Ha K-S, Kwon Y-G. p-Hydroxybenzyl alcohol-containing biodegradable nanoparticle improves functional blood flow through angiogenesis in a mouse model of hindlimb ischemia, Biomaterials 53 (2015) 679–687. [PubMed: 25890763]

[45]. Simon M, Röckl W, Hornig C, Gröne EF, Theis H, Weich HA, Fuchs E, Yayon A, Gröne HJ. Receptors of vascular endothelial growth factor/vascular permeability factor (VEGF/VPF)

in fetal and adult human kidney: localization and [125I] VEGF binding sites, Journal of the American Society of Nephrology 9 (1998) 1032–1044. [PubMed: 9621286]

[46]. Leslie JD, Ariza-McNaughton L, Bermange AL, McAdow R, Johnson SL, Lewis J. Endothelial signalling by the Notch ligand Delta-like 4 restricts angiogenesis. 2007.

[47]. Harrington LS, Sainson RC, Williams CK, Taylor JM, Shi W, Li J-L, Harris AL. Regulation of multiple angiogenic pathways by Dll4 and Notch in human umbilical vein endothelial cells, Microvascular research 75 (2008) 144–154. [PubMed: 17692341]

[48]. Suchting S, Freitas C, le Noble F, Benedito R, Bréant C, Duarte A, Eichmann A. The Notch ligand Delta-like 4 negatively regulates endothelial tip cell formation and vessel branching, Proceedings of the National Academy of Sciences 104 (2007) 3225–3230.

[49]. Hellström M, Phng L-K, Hofmann JJ, Wallgard E, Coultas L, Lindblom P, Alva J, Nilsson A-K, Karlsson L, Gaiano N. Dll4 signalling through Notch1 regulates formation of tip cells during angiogenesis, Nature 445 (2007) 776–780. [PubMed: 17259973]

[50]. Noguera-Troise I, Daly C, Papadopoulos NJ, Coetzee S, Boland P, Gale NW, Lin HC, Yancopoulos GD, Thurston G. Blockade of Dll4 inhibits tumour growth by promoting non-productive angiogenesis, Nature 444 (2006) 1032–1037. [PubMed: 17183313]

[51]. Akhurst RJ, Hata A. Targeting the TGFβ signalling pathway in disease, Nature reviews Drug discovery 11 (2012) 790–811. [PubMed: 23000686]

[52]. Pepper MS. Transforming growth factor-beta: vasculogenesis, angiogenesis, and vessel wall integrity, Cytokine & growth factor reviews 8 (1997) 21–43. [PubMed: 9174661]

[53]. Clark DA, Coker R. Transforming growth factor-beta (TGF-beta), The international journal of biochemistry & cell biology 30 (1998) 293–298. [PubMed: 9611771]

[54]. Turner M, Chantry D, Feldmann M. Transforming growth factorβ induces the production of interleukin 6 by human peripheral blood mononuclear cells, Cytokine 2 (1990) 211–216. [PubMed: 2104224]

[55]. Azhar M, Schultz JEJ, Grupp I, Dorn II GW, Meneton P, Molin DG, Gittenberger-de Groot AC, Doetschman T. Transforming growth factor beta in cardio-vascular development and function, Cytokine & growth factor reviews 14 (2003) 391–407. [PubMed: 12948523]

[56]. Liang C-C, Park AY, Guan J-L. In vitro scratch assay: a convenient and inexpensive method for analysis of cell migration in vitro, Nature protocols 2 (2007) 329–333. [PubMed: 17406593]

[57]. Guan Y, Niu H, Liu Z, Dang Y, Shen J, Zayed M, Ma L, Guan J. Sustained oxygenation accelerates diabetic wound healing by promoting epithelialization and angiogenesis and decreasing inflammation, Science Advances 7 (2021) eabj0153. [PubMed: 34452918]

[58]. Fan Z, Xu Z, Niu H, Gao N, Guan Y, Li C, Dang Y, Cui X, Liu XL, Duan Y. An injectable oxygen release system to augment cell survival and promote cardiac repair following myocardial infarction, Scientific reports 8 (2018) 1371. [PubMed: 29358595]

[59]. Dang Y, Gao N, Niu H, Guan Y, Fan Z, Guan J. Targeted Delivery of a Matrix Metalloproteinases-2 Specific Inhibitor Using Multifunctional Nanogels to Attenuate Ischemic Skeletal Muscle Degeneration and Promote Revascularization, ACS applied materials & interfaces 13 (2021) 5907–5918. [PubMed: 33506676]

[60]. Niu H, Li X, Li H, Fan Z, Ma J, Guan J. Thermosensitive, fast gelling, photoluminescent, highly flexible, and degradable hydrogels for stem cell delivery, Acta biomaterialia 83 (2019) 96–108. [PubMed: 30541703]

[61]. Guan Y, Gao N, Niu H, Dang Y, Guan J. Oxygen-release microspheres capable of releasing oxygen in response to environmental oxygen level to improve stem cell survival and tissue regeneration in ischemic hindlimbs, Journal of Controlled Release 331 (2021) 376–389. [PubMed: 33508351]

[62]. Fan Z, Fu M, Xu Z, Zhang B, Li Z, Li H, Zhou X, Liu X, Duan Y, Lin P-H. Sustained Release of a Peptide-based Matrix Metalloproteinase-2 Inhibitor to Attenuate Adverse Cardiac Remodeling and Improve Cardiac Function Following Myocardial Infarction, Biomacromolecules (2017).

[63]. Bookout AL, Cummins CL, Mangelsdorf DJ, Pesola JM, Kramer MF. High-throughput real-time quantitative reverse transcription PCR, Current protocols in molecular biology 73 (2006) 15.8. 1–.8. 28.

[64]. Van Der Voort R, Van Lieshout AW, Toonen LW, Slöetjes AW, Van Den Berg WB, Figdor CG, Radstake TR, Adema GJ. Elevated CXCL16 expression by synovial macrophages recruits memory T cells into rheumatoid joints, Arthritis & Rheumatism 52 (2005) 1381–1391. [PubMed: 15880344]

[65]. Xu Y, Fu M, Li Z, Fan Z, Li X, Liu Y, Anderson PM, Xie X, Liu Z, Guan J. A prosurvival and proangiogenic stem cell delivery system to promote ischemic limb regeneration, Acta biomaterialia 31 (2016) 99–113. [PubMed: 26689466]

[66]. Westvik TS, Fitzgerald TN, Muto A, Maloney SP, Pimiento JM, Fancher TT, Magri D, Westvik HH, Nishibe T, Velazquez OC. Limb ischemia after iliac ligation in aged mice stimulates angiogenesis without arteriogenesis, Journal of vascular surgery 49 (2009) 464–473. [PubMed: 19028053]

[67]. Yu J, deMuinck ED, Zhuang Z, Drinane M, Kauser K, Rubanyi GM, Qian HS, Murata T, Escalante B, Sessa WC. Endothelial nitric oxide synthase is critical for ischemic remodeling, mural cell recruitment, and blood flow reserve, Proceedings of the National Academy of Sciences 102 (2005) 10999–11004.

[68]. Corra U, Agostoni PG, Anker SD, Coats AJ, Crespo Leiro MG, de Boer RA, Harjola VP, Hill L, Lainscak M, Lund LH. Role of cardiopulmonary exercise testing in clinical stratification in heart failure. A position paper from the Committee on Exercise Physiology and Training of the Heart Failure Association of the European Society of Cardiology, European journal of heart failure 20 (2018) 3–15. [PubMed: 28925073]

[69]. Attar A, Mehrzadeh A, Foulad M, Aldavood D, Fallahzadeh MA, Rad MA, Khosropanah S. Accuracy of exercise tolerance test in the diagnosis of coronary artery disease in patients with left dominant coronary circulation, Indian heart journal 69 (2017) 624–627. [PubMed: 29054187]

[70]. Tang ZC, Liao W-Y, Tang AC, Tsai S-J, Hsieh PC. The enhancement of endothelial cell therapy for angiogenesis in hindlimb ischemia using hyaluronan, Biomaterials 32 (2011) 75–86. [PubMed: 20889204]

[71]. Shireman PK. The chemokine system in arteriogenesis and hind limb ischemia, Journal of vascular surgery 45 (2007) A48–A56. [PubMed: 17544024]

[72]. Yu H, VandeVord PJ, Mao L, Matthew HW, Wooley PH, Yang S-Y. Improved tissue-engineered bone regeneration by endothelial cell mediated vascularization, Biomaterials 30 (2009) 508–517. [PubMed: 18973938]

[73]. Maroni D, Davis JS. TGFB1 disrupts the angiogenic potential of microvascular endothelial cells of the corpus luteum, Journal of cell science 124 (2011) 2501–2510. [PubMed: 21693577]

[74]. Ferrari G, Cook BD, Terushkin V, Pintucci G, Mignatti P. Transforming growth factor-beta 1 (TGF-β1) induces angiogenesis through vascular endothelial growth factor (VEGF)-mediated apoptosis, Journal of cellular physiology 219 (2009) 449–458. [PubMed: 19180561]

[75]. Yang S, Xin X, Zlot C, Ingle G, Fuh G, Li B, Moffat B, de Vos AM, Gerritsen ME. Vascular endothelial cell growth factor-driven endothelial tube formation is mediated by vascular endothelial cell growth factor receptor-2, a kinase insert domain-containing receptor, Arteriosclerosis, thrombosis, and vascular biology 21 (2001) 1934–1940. [PubMed: 11742867]

[76]. Zachary I. VEGF signalling: integration and multi-tasking in endothelial cell biology, Biochemical Society Transactions 31 (2003) 1171–1177. [PubMed: 14641020]

[77]. Blanco R, Gerhardt H. VEGF and Notch in tip and stalk cell selection, Cold Spring Harbor perspectives in medicine 3 (2013) a006569. [PubMed: 23085847]

[78]. Tetzlaff F, Fischer A. Control of blood vessel formation by notch signaling, Molecular Mechanisms of Notch Signaling (2018) 319–338.

[79]. De Smet F, Segura I, De Bock K, Hohensinner PJ, Carmeliet P. Mechanisms of vessel branching: filopodia on endothelial tip cells lead the way, Arteriosclerosis, thrombosis, and vascular biology 29 (2009) 639–649. [PubMed: 19265031]

[80]. Michaelis UR. Mechanisms of endothelial cell migration, Cellular and molecular life sciences 71 (2014) 4131–4148. [PubMed: 25038776]

[81]. Takahashi T, Yamaguchi S, Chida K, Shibuya M. A single autophosphorylation site on KDR/Flk-1 is essential for VEGF-A-dependent activation of PLC-γ and DNA synthesis in vascular endothelial cells, The EMBO journal 20 (2001) 2768–2778. [PubMed: 11387210]

[82]. Olsson A-K, Dimberg A, Kreuger J, Claesson-Welsh L. VEGF receptor signalling? In control of vascular function, Nature reviews Molecular cell biology 7 (2006) 359–371. [PubMed: 16633338]

[83]. Roca C, Adams RH. Regulation of vascular morphogenesis by Notch signaling, Genes & development 21 (2007) 2511–2524. [PubMed: 17938237]

[84]. Pedrosa A-R, Trindade A, Fernandes A-C, Carvalho C, Gigante J, Tavares AT, Diéguez-Hurtado R, Yagita H, Adams RH, Duarte A. Endothelial Jagged1 antagonizes Dll4 regulation of endothelial branching and promotes vascular maturation downstream of Dll4/Notch1, Arteriosclerosis, thrombosis, and vascular biology 35 (2015) 1134–1146. [PubMed: 25767274]

[85]. Bao X, Lu C, Frangos JA. Mechanism of temporal gradients in shear-induced ERK1/2 activation and proliferation in endothelial cells, American Journal of Physiology-Heart and Circulatory Physiology 281 (2001) H22–HH9. [PubMed: 11406464]

[86]. Hoefen RJ, Berk BC. The role of MAP kinases in endothelial activation, Vascular pharmacology 38 (2002) 271–273. [PubMed: 12487031]

[87]. Xu Y, Fu M, Li Z, Fan Z, Li X, Liu Y, Anderson PM, Xie X, Liu Z, Guan J. A prosurvival and proangiogenic stem cell delivery system to promote ischemic limb regeneration, Acta biomaterialia 31 (2016) 99–113. [PubMed: 26689466]

[88]. Barani J, Mattiasson I, Lindblad B, Gottsäter A. Cardiac function, inflammatory mediators and mortality in critical limb ischemia, Angiology 57 (2006) 437–444. [PubMed: 17022379]

[89]. Lénárt N, Brough D, Dénes Á. Inflammasomes link vascular disease with neuroinflammation and brain disorders, Journal of Cerebral Blood Flow & Metabolism 36 (2016) 1668–1685. [PubMed: 27486046]

[90]. Machida S, Booth FW. Insulin-like growth factor 1 and muscle growth: implication for satellite cell proliferation, Proceedings of the Nutrition Society 63 (2004) 337–340. [PubMed: 15294052]

[91]. Nakayama KH, Shayan M, Huang NF. Engineering biomimetic materials for skeletal muscle repair and regeneration, Advanced healthcare materials 8 (2019) 1801168.

[92]. Baoge L, Van Den Steen E, Rimbaut S, Philips N, Witvrouw E, Almqvist K, Vanderstraeten G, Vanden Bossche L. Treatment of skeletal muscle injury: a review, International Scholarly Research Notices 2012 (2012).

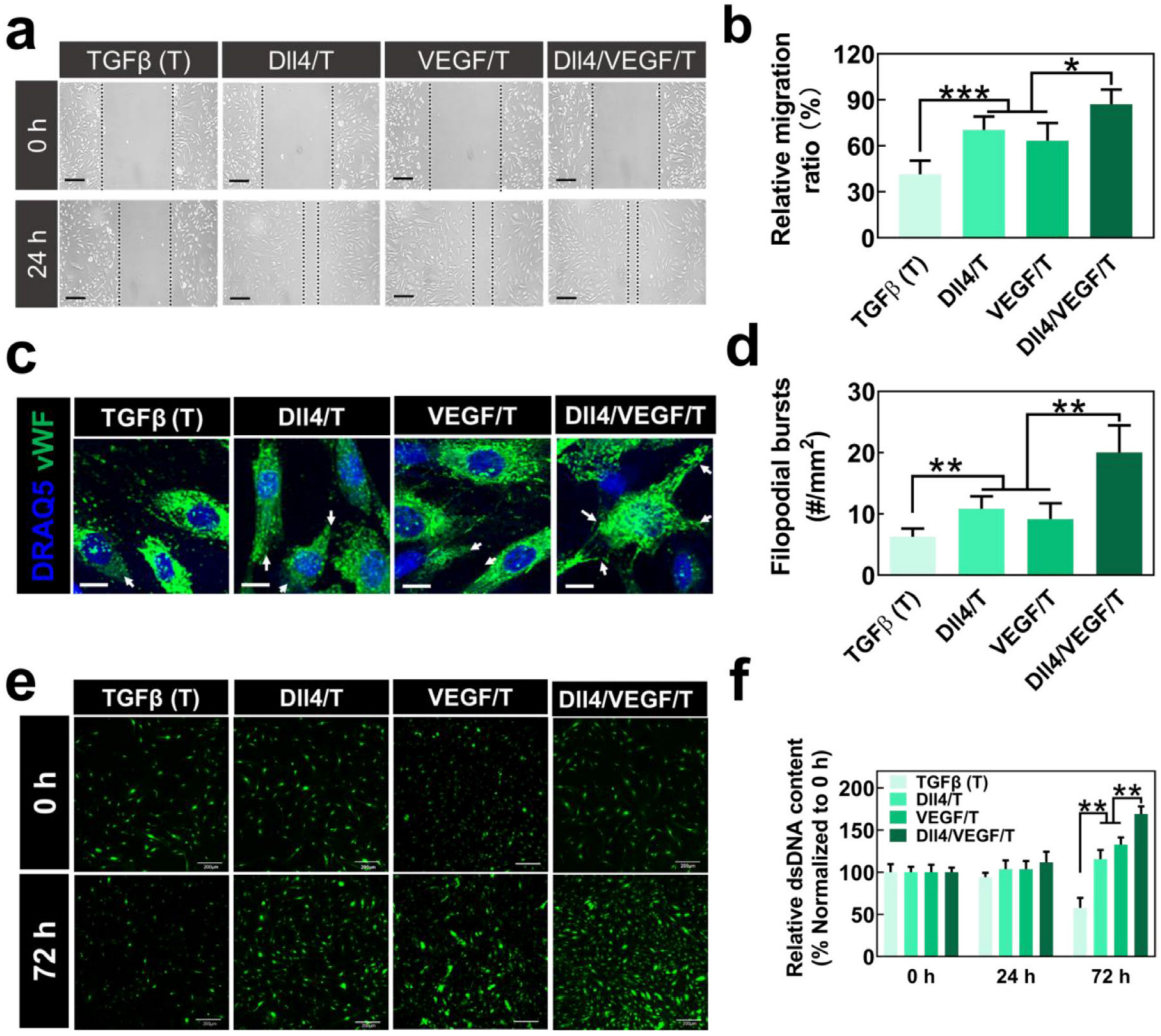

Fig. 1. Effects of Dll4 and VEGF in promoting migration and proliferation of HAECs in the presence of TGFβ.

a. Representative migration images for the groups at 0 h and 24 h. Scale bar = 100 μm. b. Quantification of relative HAEC migration ratio at 24 h (n≥6). c, d. Dll4 and VEGF increased filopodial structure formation of HAECs in the presence of TGFβ1. The cells were stained using vWF and DRAQ5. Representative images are shown in (c). Density of filopodial bursts (d) were quantified from images. Scale bar = 10 μm. e. Representative images for live HAECs at 0 and 72 h. HAECs were pre-labelled with live-cell tracker CMFDA. Scale bar = 200 μm. f. Quantification of relative dsDNA content measured by PicoGreen dsDNA (n=4). *p<0.05, **p<0.01, ***p<0.001.

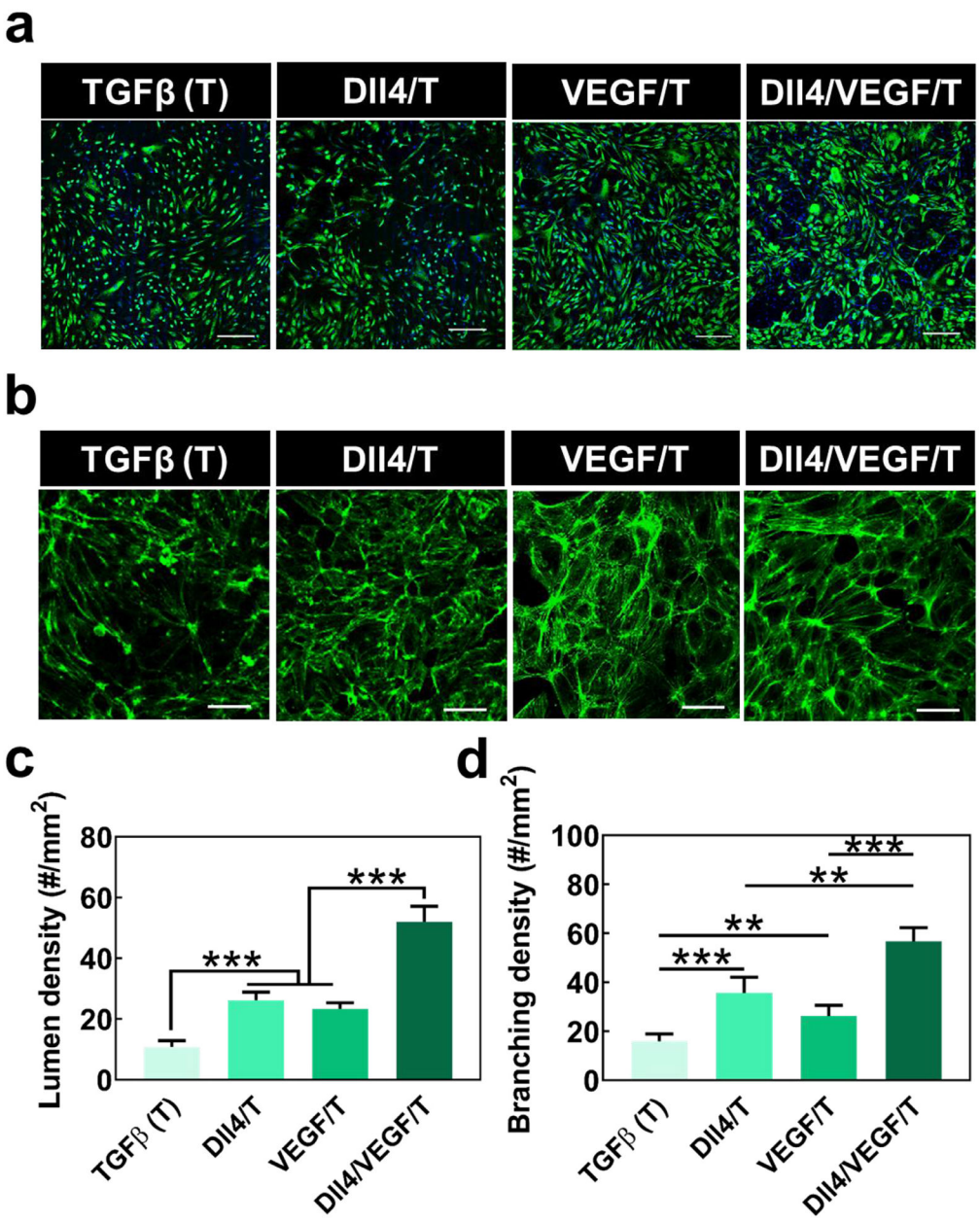

Fig. 2. Effects of Dll4 and VEGF in promoting tube formation and branching of HAECs.

a. Representative images of HAEC lumen formation on a collagen model with different treatments for 3 days in the presence of TGFβ1. Scale bar = 200 μm. b. Representative images of F-actin staining of HAECs cultured on a 3D collagen model for in vitro branching study. Scale bar = 100 μm. c. Quantification of lumen density based on images in (a). n≥4. d. Quantification of branching point density from images obtained in (b). n≥4. *p<0.05, **p<0.01, ***p<0.001.

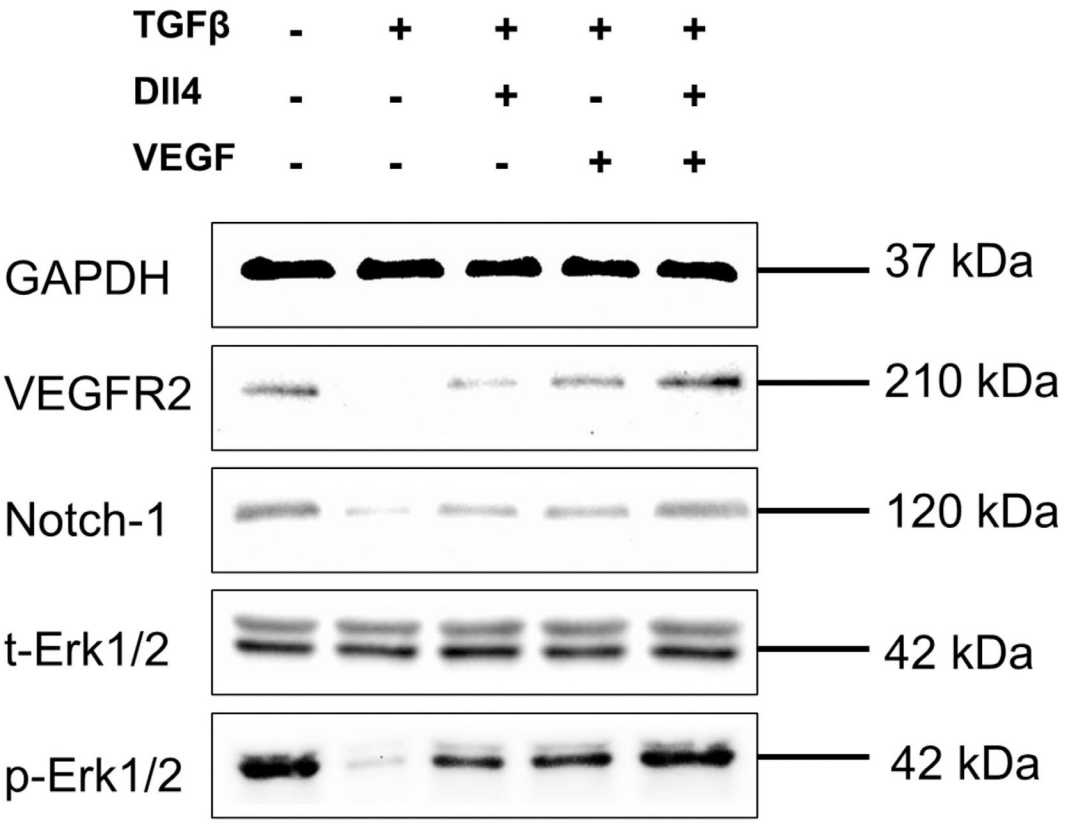

Fig. 3. Immunoblotting of VEGFR2, Notch-1, t-Erk1/2 and p-Erk1/2 in HAECs.

The cells were cultured with or without TGFβ1 for 24 hours in the presence of Dll4, VEGF or both. GAPDH serves as a loading control. The number of repetition times is 2.

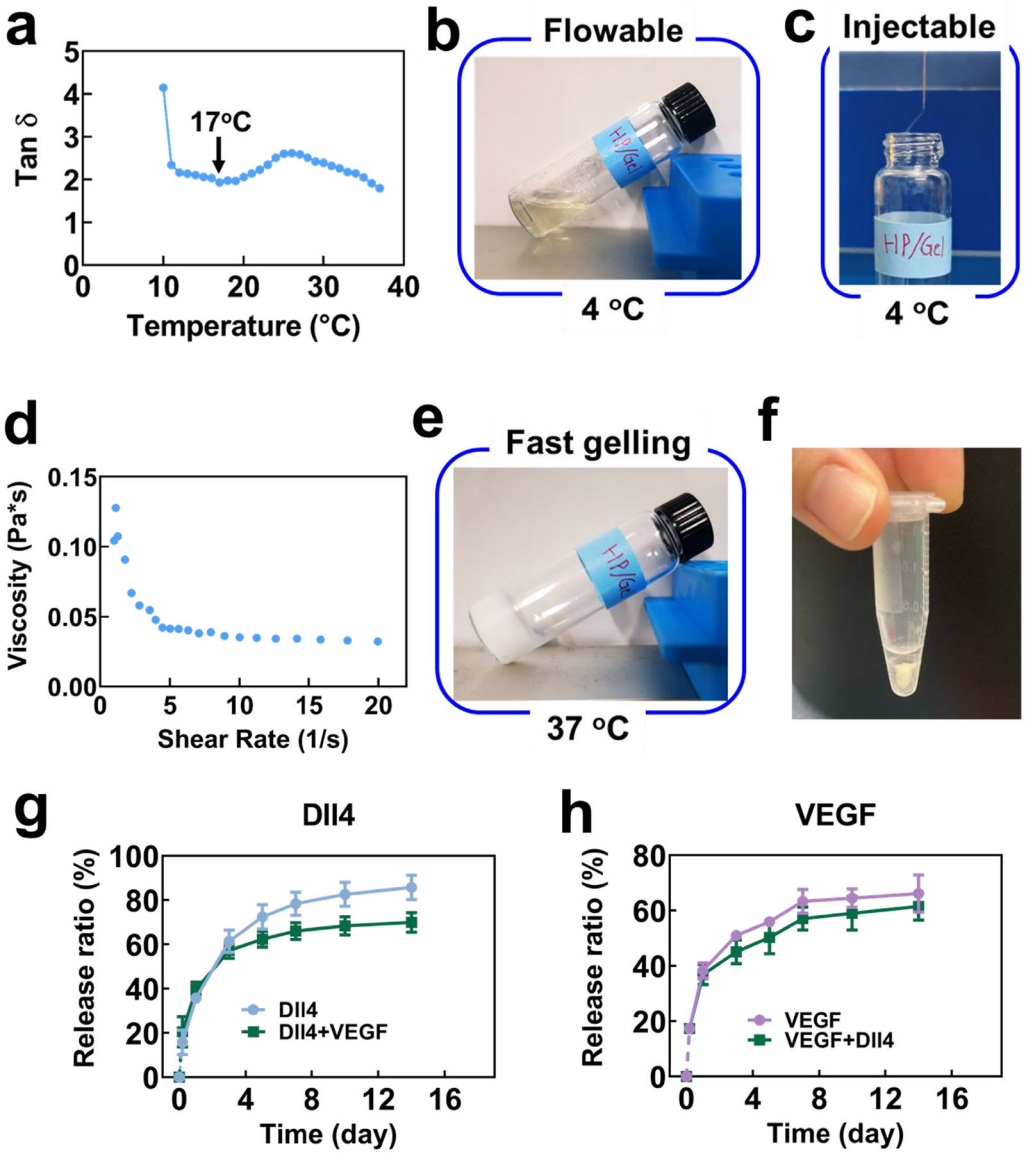

Fig. 4. Physical properties and rheological tests of the hydrogel and release kinetics of Dll4 and VEGF loaded in the hydrogel with HP for two weeks.

a. Tanδ of the hydrogel solution from 10 °C to 37 °C at a fixed strain of 2% and frequency of 1 Hz measured by rheometer. b. Flowability of the hydrogel with HP at 4 °C. c. Injectability of the hydrogel with HP at 4 °C. d. Viscosity of the 4 °C hydrogel with HP at different shear rate. e. Gelation of the hydrogel with HP at 37 °C. f. Image of the hydrogel immersed in DPBS during the release study. g, h. Cumulative ratio of Dll4 (g) and VEGF (h) in the release medium (n=6). The ratios at 4 h time point represent the growth factors not being encapsulated in the hydrogel during gelation (dash line for 0 – 4 h). The ratios after 4 h represent the growth factors released from the hydrogel after gelation (solid lines for the time points after 4 h).

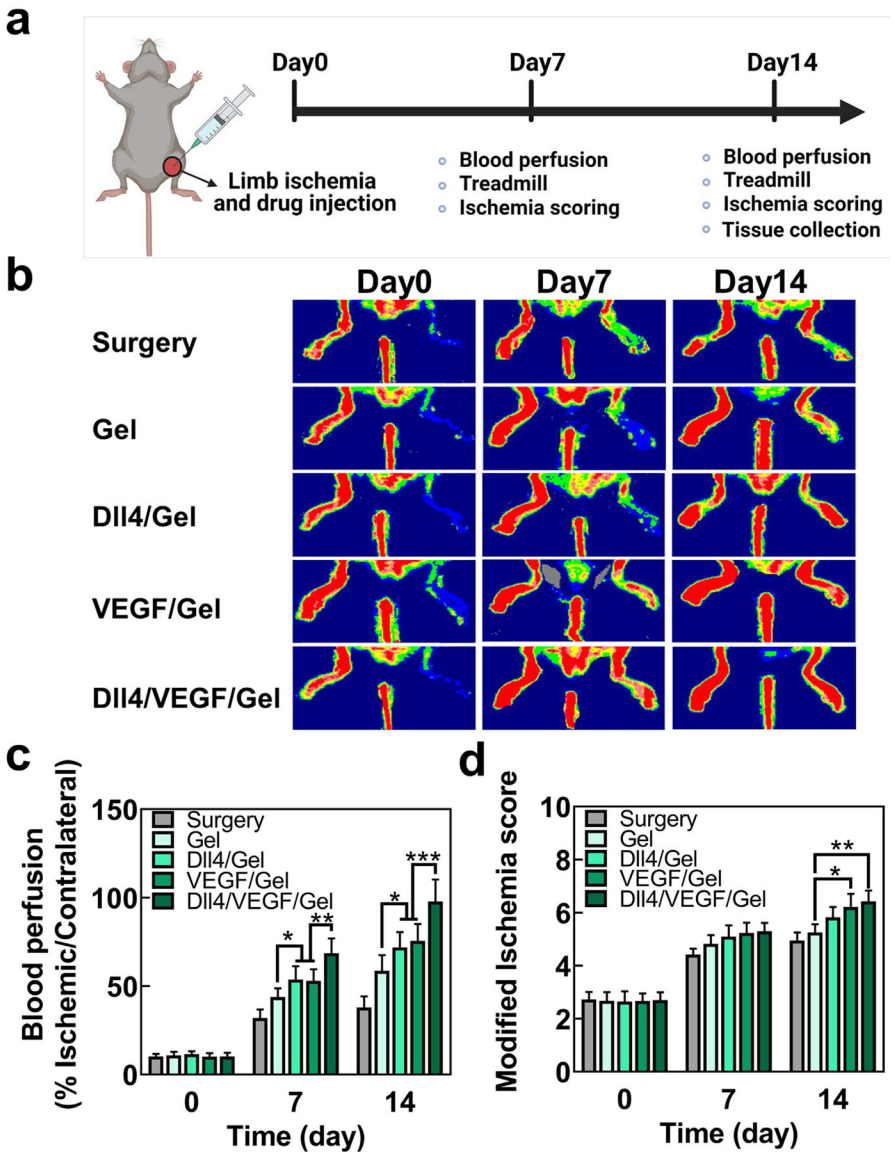

Fig. 5. Delivery of Dll4 and VEGF promoted blood perfusion in a mouse CLI model.

a. In vivo study timeline. b. Representative images of blood perfusion performed at days 0, 7 and 14 by PeriCam PSI System. c. Quantification of the relative blood perfusion ratio (blood perfusion of operated limb over contralateral limb) at days 0, 7 and 14 (n≥6). d. Modified ischemia scoring at days 0, 7 and 14 (n≥6). *p<0.05, **p<0.01, ***p<0.001.

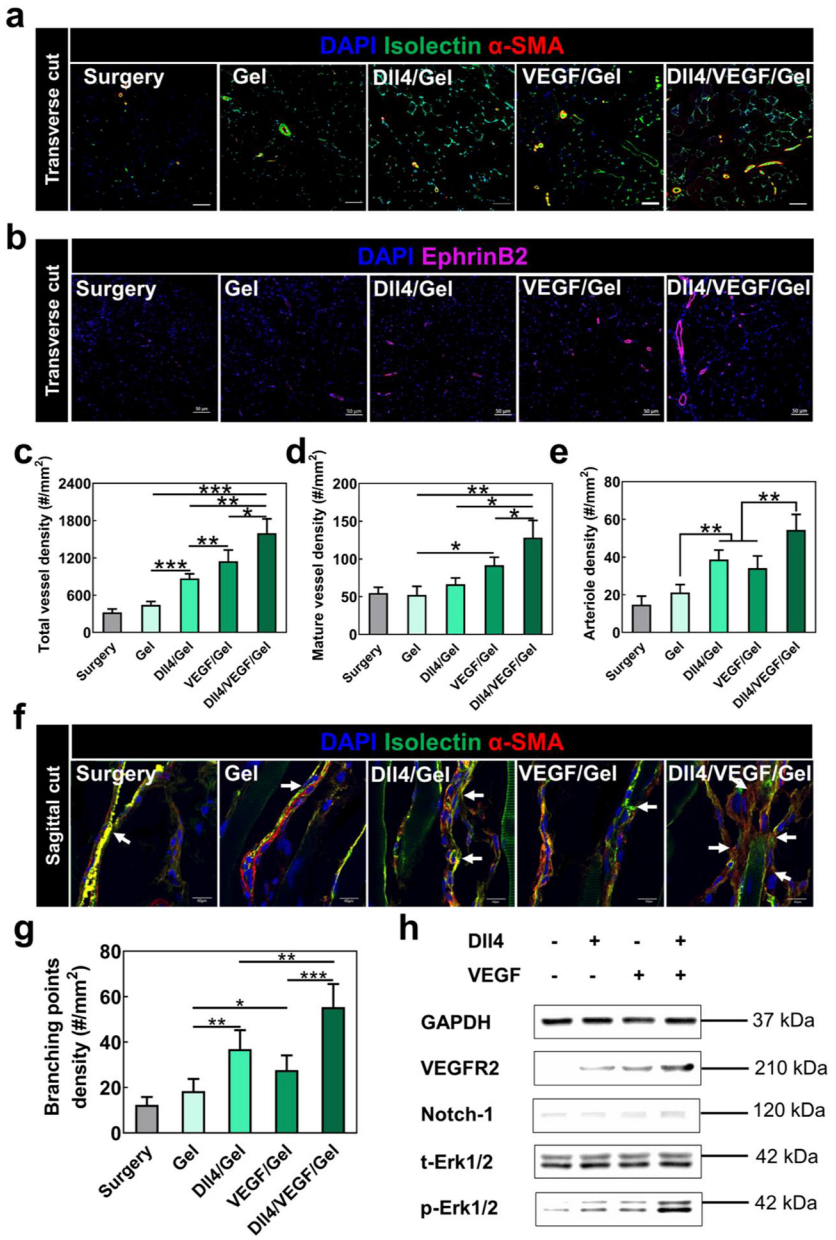

Fig. 6. Enhanced formation of blood vessels and branches by the delivery of Dll4 and VEGF.

a. Representative images of isolectin, α-SMA, and DAPI staining of ischemic limb tissues cut in transverse direction. The tissue samples were collected on day 14 post surgery. Scale bar = 50 μm. b. Representative images of EphrinB2 and DAPI staining of ischemic limb tissues cut in transverse direction. The tissue samples were collected on day 14. Scale bar = 50 μm. c. Quantification of capillary density (isolectin+) based on images in (a). n≥6. d. Quantification of mature vessel density (isolectin+ and α-SMA+) based on images in (a). n≥6. e. Quantification of arteriole density based on images in (b). n≥6. f. Representative image of isolectin and α-SMA staining of tissue samples cut in sagittal direction. The tissue samples were collected on day 14 post surgery. Scale bar = 40 μm. g. Quantification of branching point density (n≥6). h. Immunoblotting of VEGFR2, Notch-1, t-Erk1/2 and

p-Erk1/2 from the tissue lysates extracted from ischemic limb tissues harvested at day14 post-surgery. GAPDH was used as a loading control. The number of repetition times was 2. *p<0.05, **p<0.01, ***p<0.001. *p<0.05, **p<0.01, ***p<0.001.

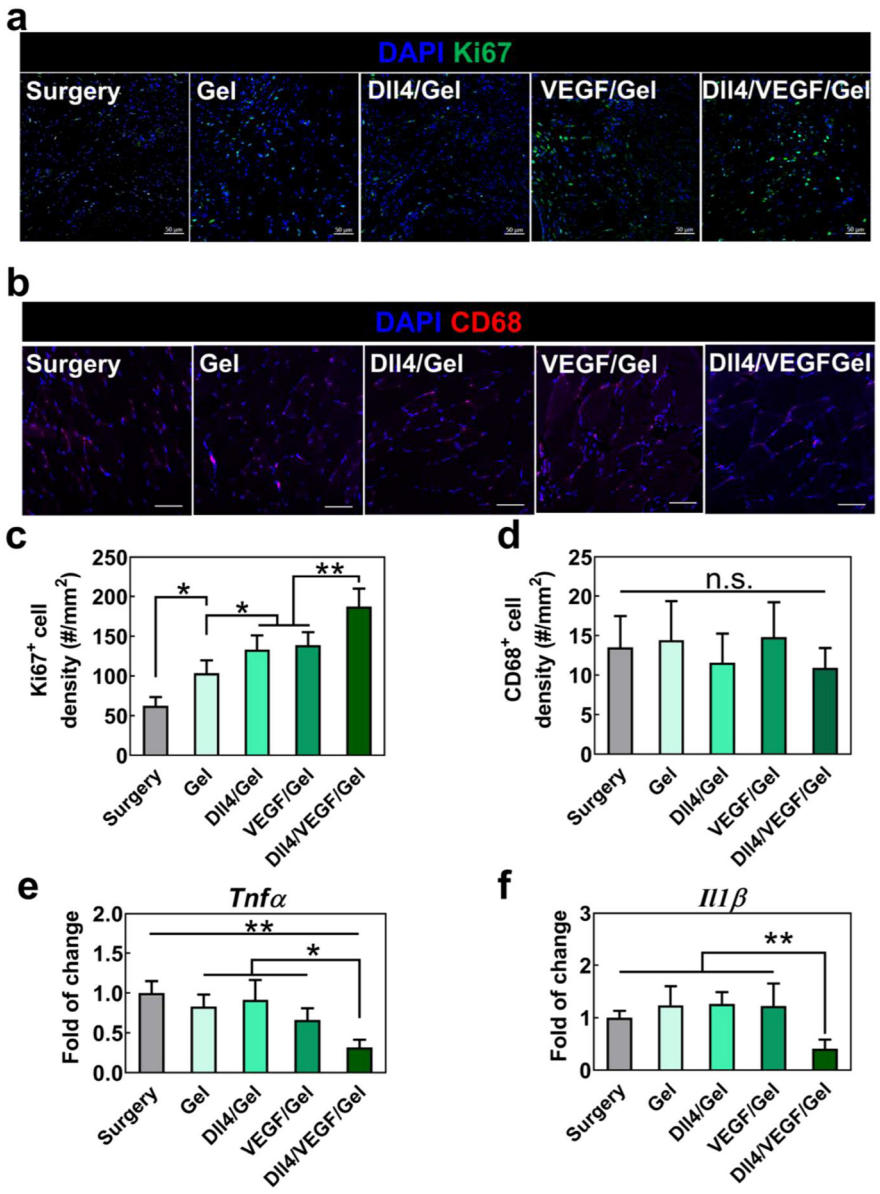

Fig. 7. Delivery of Dll4 and VEGF into ischemic limbs promoted host cell survival and did not cause substantial inflammation.

a. Representative images of Ki67 and DAPI staining of ischemic limb tissue samples collected on day 14. Scale bar = 50 μm. b. Representative images of CD68 and DAPI staining of ischemic limb tissue samples collected on day 14. Scale bar = 50 μm. c. Quantification of Ki67+ cell density based on images in (a). n=6. d. Quantification of CD68+ cell density based on images in (b). n=6. e, f. Gene expression of (e) *Tnfα* and (f) *Il1β* in ischemic limb tissues collected at 14 days post-surgery (n ≥ 4). n.s. p>0.05, *p<0.05, **p<0.01.

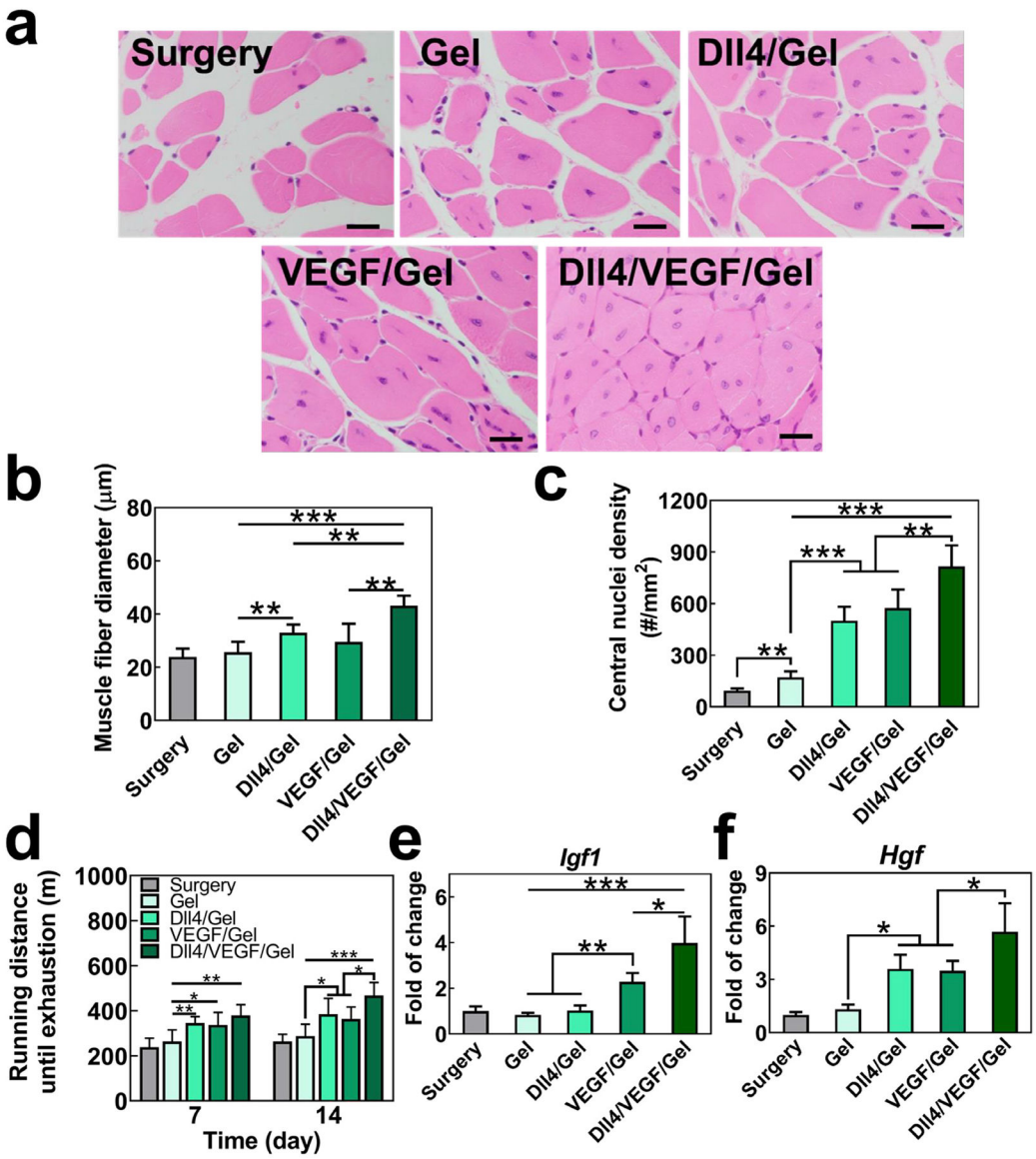

Fig. 8. Delivery of Dll4 and VEGF promoted muscle tissue regeneration and muscle function recovery.

a. Representative H&E images of ischemic limb tissue samples collected on day14. Scale bar = 20 μm. b. Quantification of muscle fiber diameter based on H&E images (n≥4). c. Quantification of central nuclei density from H&E images (n≥4). d. Evaluation of running distance until exhaustion by treadmill test at days 7 and 14 (n≥4). e, f. Gene expression of (e) *Igf1* and (f) *Hgf* from ischemic limb tissues collected at 14 days of post-surgery (n ≥ 4). *p<0.05, **p<0.01, ***p<0.001.